Eur Biophys J (1991) 19:147–155

European Biophysics Journal

Actin dynamics studied by solid-state NMR spectroscopy

L. Phillips [1], F. Separovic [2], B. A. Cornell [2], J. A. Barden [1], and C. G. dos Remedios [1]

[1] Muscle Research Unit, Department of Anatomy, The University of Sydney, N.S.W. 2006, Australia
[2] CSIRO Division of Food Processing, North Ryde, N.S.W. 2113, Australia

Received June 28, 1990/Accepted September 4, 1990

Abstract. Solid-state nuclear magnetic resonance spectroscopy was used to study the motion of ^{2}H and ^{19}F probes attached to the skeletal muscle actin residues *Cys*-10, *Lys*-61 and *Cys*-374. The probe resonances were observed in dried and hydrated G-actin, F-actin and F-actin-myosin subfragment-1 complexes. Restricted motion was exhibited by ^{19}F probes attached to *Cys*-10 and *Cys*-374 on actin. The dynamics of probes attached to dry cysteine powder or F-actin were very similar and the binding of myosin had little effect indicating that the local probe environment imposes the major influence on motion in the solid state. Correlation times determined for the solid state probes indicated that they were undergoing some rapid internal motion in both G-actin and F-actin such as domain twisting. The probe size influenced the motion in G-actin and appeared to sense monomer rotation but not in F-actin where segmental mobility and intramonomer co-ordination appeared to dominate.

Key words: Actin – Solid-state NMR spectroscopy

Introduction

Actin and myosin form the essential structural elements in the contractile apparatus in both muscle and non-muscle cells. Actin is a major component in all eukaryotic cells and is involved in processes which include cell division, cytoplasmic streaming, the maintenance of cell shape and axonal transport (Korn 1982). Filamentous or F-actin is formed when actin monomers (G-actin) polymerize. The polymer is a single-start left-handed genetic or primary helix which is strengthened by weak bonds formed between monomers on opposite strands of the two-start long pitch helix (Oosawa 1983). The conformation of the actin monomer when incorporated into the filament appears to differ from the structure adopted by the isolated monomer at low ionic strength (Barden and dos Remedios 1985; Frieden 1982; Miki et al. 1987; Vandekerckhove et al. 1985). Myosin binds very close to the N-terminal actin residues in F-actin (Sutoh 1982) although others (Miller et al. 1987) have demonstrated that residues 1–7 are not directly involved in the site. Residues 18–28 have been strongly implicated (Mejean et al. 1988) and recently, ^{19}F NMR spectroscopy was used to locate *Cys*-10 in the myosin binding site (Barden et al. 1989). Among the regions on actin involved in actin-actin binding sites is the segment 40–69 (Hambly et al. 1986). ^{1}H and ^{19}F NMR spectroscopy has shown this region to contain a residue (*Lys*-61) which is close to the groove formed between actin monomers and directly involved in both the myosin and tropomyosin binding sites (Barden and Phillips 1990).

Protein function may be critically dependent on a range of internal motions. Contractility involves some structural rearrangement and consequently, flexibility and motion may be an integral part of the force generation process. In the present study the order and dynamics of actin and the effect of binding myosin subfragment-1 (S-1) is investigated using solid state NMR spectroscopy. Both native and labeled actin were used. Several sites were labeled selectively with external chemical probes. These include *Cys*-10, *Cys*-374 and *Lys*-61 (Barden and Phillips 1990). These sites were labeled with ^{2}H probes, effective because of low natural abundance, or with ^{19}F probes which possess the additional advantage of high sensitivity. Several studies of labeled actin have been reported employing high resolution NMR (Barden et al. 1980; Barden et al. 1989; Barden and Phillips 1990; Brauer and Sykes 1981a, b; Brauer and Sykes 1986). Solid state NMR may be used to report on the restricted motion undergone by the labeled groups, although this information normally requires the prior assignment of resonances to a specific site. To this end, the solution state data (Barden et al. 1989; Barden and Phillips 1990) have enabled an interpretation to be made of the solid state data when more than one labeled site may be contributing to the observed spectrum.

Materials and methods

Probe preparations

Two probes, 3-bromo-1,1,1,-trifluoropropanone (BTFP) and pentafluorophenylisothiocyanate (PFPITC) were obtained from Tokyo Kasei and Fluka respectively. The (trifluoromethyl)mercuric bromide (CF_3HgBr) (Barden et al. 1989) and d_5-tryptophan preparations (Matthews et al. 1977; Kinsley et al. 1981) were as described previously. The d_2-iodoacetamide (d_2-IAA) was prepared by chlorinating deuterated acetic acid followed by esterification with ethanol. The chloroacetate was reacted with ammonia to form chloroacetamide (Jacobs and Heidelberger 1932; Vogel 1979). The chlorine was exchanged for iodine in the final product. Red phosphorus (0.21 g) and CD_3COOD (5.25 g) were added to an oven-dried 3-neck 25 ml flask fitted with a gas inlet from a cylinder of Cl_2 gas. The outlet was attached to a series of three scrubbing bubblers. An oil bath was heated to 104 °C, then the apparatus was lowered in and the contents stirred magnetically. The Cl_2 flow was commenced and the reaction vessel illuminated with eight 20 W fluorescent lamps. The attached condensor was cooled with ethanol to −70 °C to prevent loss of the CD_3COOD vapour. After 6 h, the flask was cooled and the product allowed to crystallize overnight. Two distallations through an air condensor (bp 184–192 °C) yielded white crystals of d_3-monochloroacetic acid (92% yield). A total of 3.0 g (31 mmol) of the d_3-chloroacetic acid and 2.9 ml (41 mmol) of distilled $SOCl_2$ were added under a N_2 atmosphere. The apparatus with attached dropping funnel was heated to 110 °C to melt the $ClCD_2COOD$ with the $SOCl_2$ added dropwise over 15 min, producing a vigorous evolution of HCl. The reaction vessel was stirred for 75 min. After cooling, the reaction mixture was distilled and the fraction boiling between 102–108 °C collected. The d_2-chloroacetyl chloride (2.55 g) was formed with a yield of 71%. All of the chloride (22 mmol) was added dropwise over 30 min to a 10 ml flask with an attached dropping funnel containing 1.02 g of dry alcohol (22 mmol). This resulted in an evolution of gas. Both chloride and the stirred alcohol were cooled with ice and the apparatus placed under a N_2 atmosphere. The solution was stirred for 45 min and then distilled. The fraction boiling at 142–146 °C was collected. This product was d_2-ethyl chloroacetate (1.73 g) representing a yield of 63%.

The final intermediate was prepared by mixing precooled amounts of the chloroacetate (1.45 g) with 1.5 ml of ammonia while stirring. The reaction occurred as the temperature was increased to 20 °C. A white precipitate formed consisting of d_2-chloroacetamide. A further 1.5 ml aliquot of ammonia was added and the mixture stirred for 1 h after which the product was filtered and dried. A yield of 72% was obtained. This product was refluxed with NaI in acetone under N_2 for 1 h. The cooled solution was evaporated to dryness and recrystallized from ethyl acetate and then from water to yield long colourless crystals of d_2-iodoacetamide (mp 92 °C).

Preparation of d_3-*o*-methylisourea (d_3-OMI) followed a modification of the method of Kurzer and Lawson (1963). 15 g of $CaCN_2$ (Tokyo Kasei) were added to a mortar containing glacial acetic acid and ground to a fine paste. Acid and water were added to maintain an acidic paste which was then dried for 48 h at 35 °C and 30 mm Hg. The grey powder was pulverized and extracted in a Soxhlett apparatus using water-washed ether acidified with a few drops of acetic acid. After two extractions, the ether was dried with anhydrous $NaSO_3$, and the product filtered and evaporated to dryness to yield 6.6 g of NH_2CN (84% yield). HCl gas was bubbled into a flask containing 2 g of the NH_2CN and 4 ml of CD_3OD (Sigma) for 40 min. The reaction mixture was allowed to crystallize for a few days before being filtered under N_2 and recrystallized from methanol to produce d_3-*o*-methylisourea hydrochloride (0.77 g) with a yield of 14%. A mp of 134–136 °C was measured and a single resonance at 4.79 ppm (downfield from TSS) recorded in the ^1H NMR spectrum. Rigid lattice spectra obtained from these probes required rigorous drying of the samples.

Protein preparations

Actin was prepared with very high yield (Barden et al. 1986a) from rabbit muscle acetone powder. Labeling of actin with d_2-IAA was achieved using F-actin (2.2 g) in 0.1 *M* KCl, 1 m*M* ATP, 1 m*M* NaN_3, 2 mg/L leupeptin, 2 mg/L chymostatin, 10 mg/L TLCK, 1 *M* urea and 20 m*M* $NaPO_4$ (pH 7.0) to which was added a 10-fold molar excess of d_2-IAA. The reaction vessel was enclosed in foil and the solution was stirred for 12 h at 20 °C. The labeled actin was centrifuged at 100 000 g for 1.5 h at 17 °C and then the pellets of F-actin were homogenized in 0.4 m*M* ATP, 0.2 m*M* $CaCl_2$ and 1 m*M* Tris (pH 8.0). The actin (4 mg/ml) was dialyzed for 30 h at 4 °C against a similar low ionic strength buffer containing ammonium formate (pH 8.0) with a total of five changes of dialysate. The actin was clarified at 100 000 g for 1.5 h at 4 °C and lyophilized. The lyophilized G-actin was washed with deuterium-depleted water (Sigma) and lyophilized several times to remove traces of exchangeable deuterium. The ^2H NMR spectra were recorded using both dry and hydrated G-actin. Preparation of ^{19}F-labeled actin was accomplished using BTFP (Barden et al. 1989), CF_3HgBr (Barden et al. 1989) and PFPITC (Barden and Phillips 1990). Lyophilized protein samples, rehydrated powders and centrifuged pellets of actin and actin-subfragment-1 complexes were used. Myosin was extracted from rabbit muscle (Tonomura et al. 1966) and subfragment-1 was prepared according to the method of Weeds and Taylor (1975).

NMR spectroscopy

Spectra were recorded on a Bruker CXP-300 NMR spectrometer operating at 282.23 MHz for ^{19}F, 75.46 MHz for ^{13}C and 46.05 MHz for ^2H. Proton-enhanced ^{13}C spectra (Pines et al. 1973) were obtained at 283 K with a contact time of 1 ms, ^1H $\pi/2$ pulse of 5 μs and a repetition rate of 2 s. A sweep width of 62.5 kHz was employed with 1024

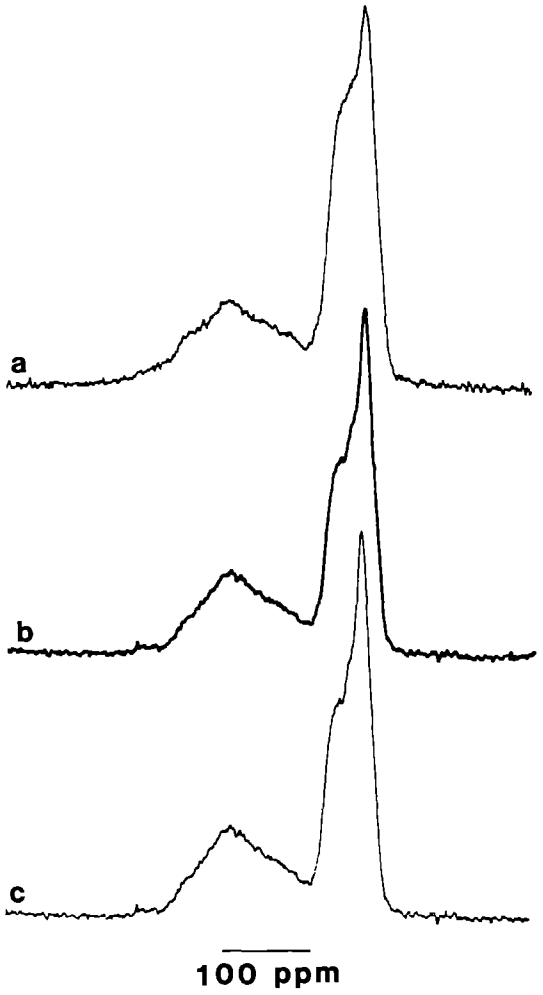

Fig. 1. ^{13}C NMR spectra of: (a) lyophilized G-actin after 36 000 scans; (b) lyophilized F-actin after 6000 scans; and (c) a hydrated pellet of F-actin after 28 000 scans. A line broadening of 50 Hz has been applied

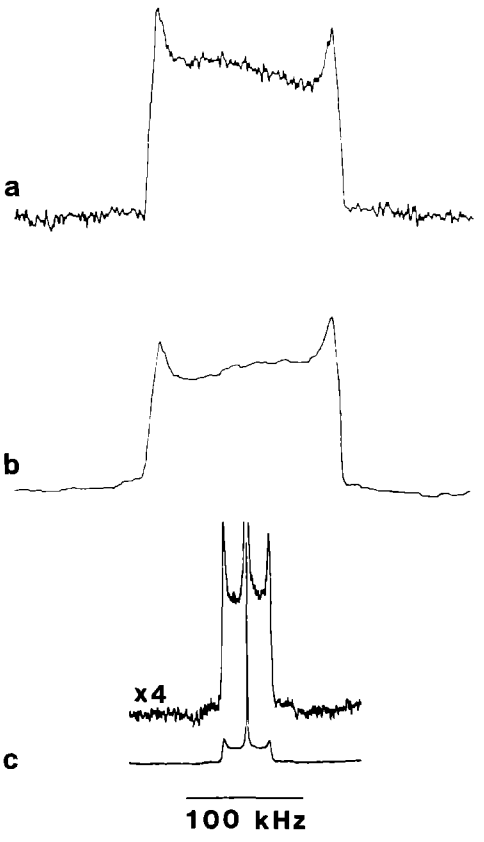

Fig. 2. ^{2}H NMR spectra of: (a) tryptophan powder after 22 000 scans; (b) iodoacetamide powder after 550 scans; and (c) ortho-methyl isourea powder after 10 000 scans. A 4-fold expansion of spectrum (c) is shown

data points. ^{19}F and ^{2}H spectra were acquired using a solid echo pulse sequence $(90_x - \tau - 90_y)$ with τ of order 50 μs, 1024 data points and a sweep width of 1 MHz for ^{2}H and 62.5 kHz for ^{19}F. The $\pi/2$ pulse for ^{2}H was 4 μs and for ^{19}F it was 8 μs. T_1 values were determined using the inversion recovery technique and the T_2 from varying the delay using the solid echo sequence. Samples were placed in 10 mm NMR tubes and run at 10–15 °C unless specified otherwise. Control ^{19}F spectra were recorded using unlabeled actin and both the ^{2}H depleted water and native actin were checked to ensure they gave no ^{2}H signal.

Results

Native actin was studied by ^{13}C NMR spectroscopy in the form of lyophilized G-actin and as a hydrated F-actin pellet. Attempts to study a solution of G-actin produced a poor signal to noise ratio due to a combination of the low actin concentration that had to be maintained to inhibit polymerization (ca. 4 mg/ml) and to the inefficient C–H cross-polarization for the G-actin solution. The ^{13}C spectra shown in Fig. 1 revealed broad resonances from both aliphatic and backbone carbonyl groups indicating that actin has an essentially rigid backbone in both the lyophilized G-actin form (Fig. 1 a) and lyophilized F-actin form (Fig. 1 b). No detectable change was observed upon hydration of the F-actin (Fig. 1 c) indicating that the global order of the carbonyl backbone remains unaffected by hydration. However, site specific probes were able to detect localized changes in motion within the protein.

Rigid lattice spectra of some dry probes are shown in Fig. 2 for d_5-tryptophan (Fig. 2 a), d_2-IAA (Fig. 2 b) and d_3-OMI (Fig. 2 c). These provide a reference for the order experienced by these probes when bound to actin. Spectra in Fig. 2 a and b are similar with a peak separation of 160 and 170 kHz respectively, while the spectrum of d_3-OMI (Fig. 2 c) has a separation of 43 kHz. Actin was labeled with d_2-IAA at *Cys*-10 and *Cys*-374 (Barden et al. 1986 b). The extent of labeling was determined by a sulfhydryl assay (Habeeb 1972) and by solid state ^{2}H NMR. Spectra recorded from lyophilized G-actin showed that the d_2-IAA probes produced a resonance with a width of 150–160 kHz (Fig. 3 a) suggesting that the probes were undergoing a two-fold flip (Spiess 1984). Hydration of the d_2-IAA actin with deuterium-depleted water resulted in the single broad resonance collapsing into a two-component spectrum comprising a narrow resonance (3 kHz) located above a much broader resonance (Fig. 3 b). The

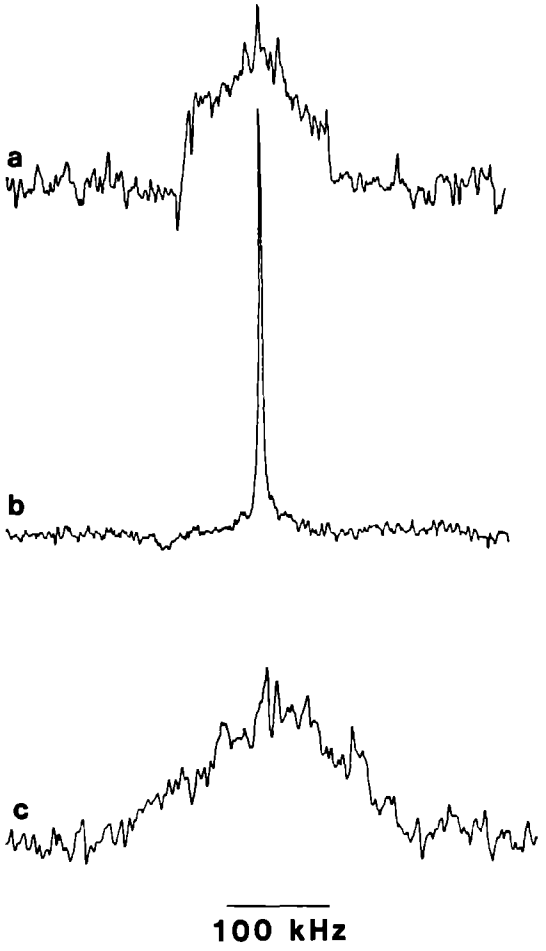

Fig. 3. ^{2}H NMR spectra of: (**a**) a dry powder sample of iodoacetamide-actin after 140 000 scans at 7 °C; (**b**) a hydrated pellet of iodoacetamide-actin under identical conditions which is motionally narrowed; and (**c**) a hydrated pellet of the IAA-actin after 55 000 scans showing only a broad component at −81 °C. The line broadening is 200 Hz

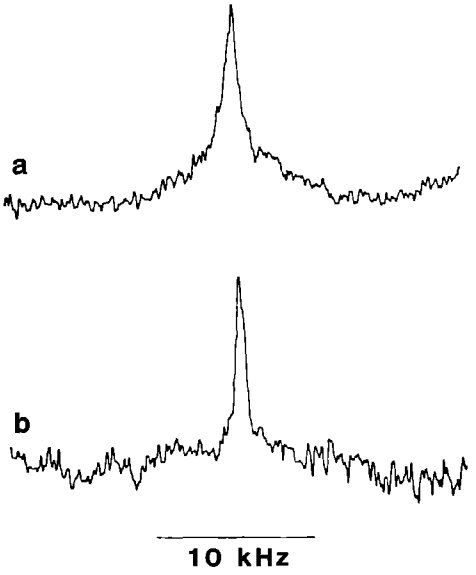

Fig. 4. ^{19}F NMR spectra of: (**a**) a BTFP-actin pellet after 3250 scans at 5 °C; and (**b**) a BTFP-actin-S1 pellet after 26 800 scans. The line broadening is 100 Hz

intensity of the narrow resonance is approximately 25% of the intensity of the broad resonance at 7 °C. A comparison was made with unlabeled actin treated similarly. In this case, a narrower signal was recorded with less than 5% of the total intensity. This residual resonance probably arises from the natural abundance of HOD in the water of hydration. An axially symmetric pattern corresponding to a quadrupolar splitting (Sarkar et al. 1987) of 180 kHz resulted when the labeled actin pellet was frozen over the temperature range −17 °C to the lowest value recorded at −81 °C (Fig. 3c).

In order to improve the signal/noise ratio, a series of fluorine labels were prepared and studied using ^{19}F NMR spectroscopy. The much more sensitive spin 1/2 ^{19}F nucleus does not occur naturally in actin. It has spectral characteristics dominated by homonuclear and heteronuclear dipolar coupling and chemical shift anisotropy. Measurements of probe order through the use of the static ^{19}F dipolar and ^{2}H quadrupolar interactions were complemented by relaxation measurements to determine the timescale of the motion. BTFP has been used to study the dynamics of actin (Brauer and Sykes 1986). In the present work, BTFP was attached to the amino acid cysteine and used to obtain a measurement of the dynamics of the dry probe. A linewidth of 3.3 kHz at half height was measured. Difficulties encountered in attaching the CF_3 probe to the actin have been discussed (Barden et al. 1989). Sulfhydryl determinations on BTFP-actin revealed that substantial blocking had occurred. Preliminary studies of G-actin labeled with BTFP indicated that the CF_3 group readily dissociated upon lyophilization (Barden et al. 1989). The samples prepared with the ^{19}F probes were isolated as F-actin or F-actin-S1 complexes and were centrifuged into fully hydrated pellets at ca. 0.5 g/ml. Spectra recorded from BTFP-F-actin and BTFP-F-actin-S1 complex are shown in Fig. 4a and b respectively. The spectrum in Fig. 4a exhibits a sharp resonance with a width at half height of 1.0 kHz superimposed on a broader resonance (4.5 kHz). Relaxation times for this hydrated sample were very similar to those recorded from the BTFP-labeled cysteine as a dry powder (Table 1). The broad underlying component may have been influenced by the binding of myosin S1 (Fig. 4b). A solution state NMR study has demonstrated that the *Cys*-374 resonance is broadened beyond detection by polymerization to F-actin (Barden et al. 1989) but the greater bandwidth in the solid state spectrum permits detection of a resonance even arising from an immobilized probe. Actin polymerization may influence the dynamics of F-actin significantly by causing a reduction in the molecular tumbling rate which enables the detection of a high-resolution NMR signal. The high-resolution solution state NMR study showed that the *Cys*-10 resonance is broadened by S1 binding (Barden et al. 1989). These studies enabled the narrow resonance in Fig. 4 to be assigned to *Cys*-374. From the present study we conclude *Cys*-374 is located in a less ordered surface accessible environment close to an actin-actin interaction site whereas *Cys*-10, near the S1 binding site (Barden et al. 1989), is more ordered and thus gives rise to the broader resonance (Seiter and Chan 1973). The difference in the

Table 1. Spin-lattice and spin-spin relaxation time measurements for a range of probes considered for incorporation into actin

Sample	T_1 (s)	T_{2e} (μs)	τ_s (s) from T_{2e}
BTFP-*Cys*- (dry)	0.45	175	1.4×10^{-5}
BTFP-F-actin	0.50	300	7.9×10^{-6}
BTFP-F-actin-S1	0.50	300	7.9×10^{-6}
CF_3Hg-*Cys* (dry)	0.77	(*i*) 110	1.3×10^{-5}
		(*ii*) 2100	6.8×10^{-7}
(wet)	1.50	(*i*) 440	3.3×10^{-6}
		(*ii*) 1.25×10^5	1.1×10^{-8}
CF_3HgBr (wet)	2.50	3.80×10^5	3.6×10^{-9}
CF_3Hg-G-actin	0.65	3.70×10^5	3.7×10^{-9}
CF_3Hg-F-actin	0.70	200	7.2×10^{-6}
CF_3Hg-F-actin-S1	0.50	150	9.6×10^{-6}
PFPITC-*Lys* (dry)	0.68	2100	3.8×10^{-6}
(wet)	0.51	(*i*) 400	2.0×10^{-5}
		(*ii*) 7.50×10^4	1.1×10^{-7}
PFPITC-F-actin	0.75		

(*i*) and (*ii*) refer to the fast and slow components of T_2. A double exponential decay was evident for these samples

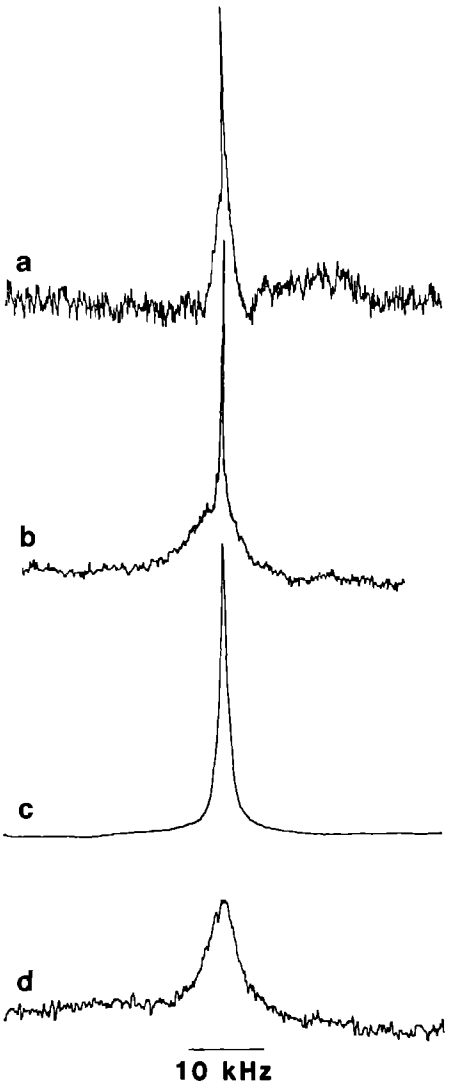

Fig. 5. ^{19}F NMR spectra of: (**a**) CF_3Hg-F-actin pellet with a label ratio of 0.6 after 45 000 scans; (**b**) CF_3Hg-F-actin pellet with a label ratio of 2.1 after 27 000 scans; (**c**) unpolymerizable CF_3Hg-G-actin with a label ratio of 4.8 after 34 000 scans; and (**d**) pellet as described in spectrum (**b**) but with myosin S-1 bound to the actin, after 55 000 scans. The temperature is 15 °C and the line broadening is 100 Hz

segmental motion of the actin backbone in these two regions was undetectable using the narrow spectral bandwidth of the high-resolution study. When the actin was frozen and thus denatured, the broad resonance disappeared. This observation is consistent with the *Cys*-10 resonance being associated with a structured environment. The broad component was not evident in the S1-bound complex (Fig. 4b). These samples produced pellets that were softer than F-actin and consequently the signal concentration was lower. It is thus possible that the broad component may be buried within the noise.

The CF_3HgBr probe was synthesized to overcome the lability problem associated with BTFP (Barden et al. 1989). The stability of the CF_3Hg probe was enhanced by using chloride free solutions (Bendall and Lowe 1976). The small size and high affinity of the probe for the cysteines on actin enabled almost stoichiometric labeling of the actin. Labeling of more than 3 sites prevented actin polymerization, thereby allowing an investigation of a hydrated G-actin to be made at a high concentration (60 mg/ml). The CF_3 Hg group was attached to cysteine powder (CF_3-*Cys*) and examined in both the dry and hydrated from as a control for the protein-labeled spectra. Linewidths at half height of 1.4 and 0.6 kHz respectively, were recorded.

^{19}F NMR spectra of CF_3Hg-actin in Fig. 5 were recorded at label ratios of (**a**) 0.6; (**b**) 2.1; (**c**) 4.8, an unpolymerizable actin sample; and (**d**) 2.1 in the presence of S1. The ratios were determined from sulfhydryl assays. From the results of earlier work (Barden et al. 1989), the sample (**a**) contains label attached only to *Cys*-374 and the sample (**b**) contains label attached to both *Cys*-374 and *Cys*-10. The *Cys*-374 resonance appears as the narrow signal in Fig. 5a while the *Cys*-10 resonance is the broad peak underlying the narrow resonance in Fig. 5b. The narrow *Cys*-374 resonance was observed to decline in intensity over a period of several hours apparently due to the reversible progressive ionic cross-linking of the filaments. This process results in a more constrained polymeric structure which alters label accessibility and segmental mobility, properties which are the determinants of the resonance line width. This cross-linking has been observed in an EPR study (Mossalowska et al. 1988) and has been discussed recently in regard to the stability of the actin filament (Erickson 1989). The binding of S1 to the actin sample used in Fig. 5b results in the spectrum shown in Fig. 5d. There is no evidence of the narrower component in the spectrum of the complex. Denaturation of the actin caused by the binding of the label to all the *Cys* residues results in the spectrum of Fig. 5c. This shows the presence of a single peak with a linewidth of 1 kHz and is a superposition of the resonances from all the *Cys* sites. The restricted motion undergone by the F-actin samples compared to the G-actin sample in Fig. 5c is evident from the greater than 1000-fold difference in the T_2 (see Table 1) value.

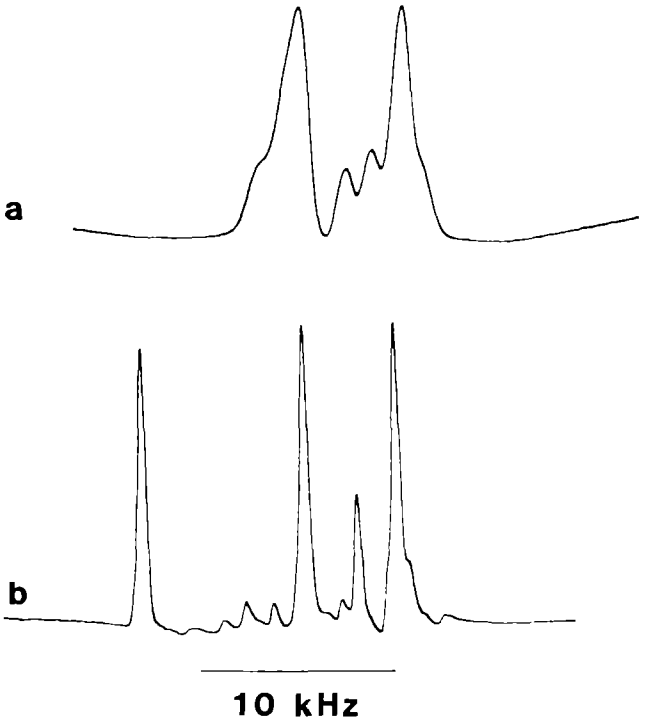

Fig. 6. ^{19}F NMR spectra of: (**a**) dry PFPITC-lysine powder after 500 scans; and (**b**) a wet sample after 50 scans. A breakdown product appears in the motionally-narrowed wet spectrum downfield of the main resonances. The line broadening is 20 Hz

The behaviour of the BTFP and CF_3Hg probes bound to actin differs in the presence of S1. The BTFP resonance appears to narrow while the CF_3Hg signal remains broad. The former may be explained by a decrease in the order of the more flexible carbon linkage to the sulfhydryl group. The CF_3Hg has the CF_3 directly attached to the sulfhydryl by a metal and would be expected to be more linear and rigid. The slightly shorter T_2 of the mercury probe probably reflects its greater order arising from the Hg linkage.

At the very high actin samples used in this study, no significant amount of G-actin remained in the rehydrated actin gel, having been removed prior to preparation of the gel samples. The actin-activated myosin ATPase activities of the BTFP and CF_3-labeled actin containing up to 2 labels/actin were indistinguishable from the unlabeled actin samples.

In order to investigate the effects of steric hindrance, a larger probe (PFPITC) was used to label *Lys*-61 as reported in an earlier high-resolution study (Barden and Phillips 1990). A preliminary investigation of the solid state spectrum of PFPITC-actin was made. Figure 6 shows spectra of PFPITC attached to the amino acid lysine both in the dry and hydrated forms. The non-equivalent ortho, meta- and para fluorines also could be discerned in the PFPITC-actin spectrum with an increased linewidth being evidence for a restricted motion of the probe. The labeled hydrated F-actin and the dry PFPITC-*Lys* powder spectra show similar relaxation properties and linewidths, in common with the spectra obtained from the other ^{19}F-labeled probes.

Relaxation measurements

The rigid-rotor model of anisotropic motion (Woessner 1962; Doddrell et al. 1972) for homonuclear dipole coupling was adapted for the CF_3 groups used in these studies. The linewidth and spectral features present in the dipolar powder spectrum of a methyl rotor have been described theoretically (Andrew and Bersohn 1950; Seiter and Chan 1973) as an infinitely sharp spike comprising 50% of the spectral intensity at the midpoint of a rigid lattice background (Fig. 2c). The dipolar splitting is motionally narrowed when the rotor experiences restricted motion about its C_3 axis (Seiter and Chan 1973). The probe order also affects the splitting. This can be visualized as the degree of libration of the CF_3 cone about the C_3 axis. The values of T_1, T_2 and the correlation times derived from them are presented in Table 1. The relation between a laboratory frame spin-lattice relaxation time (T_1) and a molecular rotation correlation time (τ_f) is given by (Woessner 1962; Forsen and Lindman 1981):

$$1/T_1 = 9\gamma^4\hbar^2/10r^6\{[\tau_f/(16+\omega_0^2\tau_f^2)]+[\tau_f/(4+\omega_0^2\tau_f^2)]\} \quad (1)$$

for an anisotropically tumbling molecule undergoing internal reorientation. γ is the gyromagnetic ratio of the NMR probe nucleus (2.5164 $rads^{-1}\,T^{-1}$ for ^{19}F); r is the F–F distance 0.204 mm for CF_3HgBr based on a reported C–F distance of 0.125 nm (Kamenar et al. 1982), 0.222 nm for BTFP based on the C–F distance of 0.135 nm reported for trifluoroacetic acid (Sutton 1958) or 0.272 nm for PFPITC based on the structure of $C_6H_2F_4$ (Sutton 1958); ω_0 is the spectrometer frequency ($282\times2\pi\times10^6$ $rads^{-1}$); $\hbar = h/2\pi$; and τ_f is the fast correlation time which dominates T_1 relaxation.

The minimum values of T_1 derived from (1) are 0.8 and 1.5 s for CF_3Hg and BTFP respectively, yielding nanosecond correlation times. The T_1 times for F-actin and F-actin-S1 complex are of the order 0.5–0.8 s. Fluctuations in the chemical shift anisotropy may contribute to the relaxation, but only to a small extent as evidenced by the weak field dependence of the relaxation times (Barden et al. 1989). Of much greater significance is the heteronuclear dipole coupling to surrounding protons (Post et al. 1984).

Recourse was made to the spin-spin or transverse relaxation time T_2 for the derivation of the correlation time τ_s for the actin-bound CF_3 group. Using Woessner's expression for T_2 in terms of slow and fast correlation times (τ_s and τ_f) we find that terms in τ_f are negligible compared to those in τ_s. The simplified expression (Woessner 1962) is:

$$1/T_2 = 9\gamma^4\hbar^2/8r^6\{\tau_s/10+\tau_s/[6(1+\omega_0\tau_s^2)] + \tau_s/[15(1+4\omega_0^2\tau_s^2)]\} \quad (2)$$

The results are presented in Table 1.

Discussion

The correlation times determined in Table 1 should be compared with the correlation times for overall tumbling of both the G-actin monomer and an average-length

Table 2. Linewidths at half height of probe resonances. Chemical shifts are referenced to TFA

Probe	Condition	Linewidth at half height	Chemical shift
d_5-tryptophan	rigid lattice	160 kHz (90° edge splitting)	
d_2-IAA	rigid lattice	165 kHz (90° edge splitting)	
	attached to dry actin	155 kHz (90° splitting)	
	attached to wet actin	3 kHz (280 K); 160 kHz (190–256 K)	
BTFP	BTFP-*Cys*	4.5 kHz	−9 ppm
	BTFP-F-actin	1.1 ± 0.2 kHz with 5 kHz underlying component	−9 to −10 ppm
	BTFP-F-actin-S1	0.8 ± 0.1 kHz	
CF_3HgBr	rigid lattice	1.6 kHz	42 ppm
	wet probe	0.6 kHz	
	CF_3Hg-*Cys* (dry)	1.5 kHz	
	CF_3Hg-*Cys* (wet)	0.6 kHz	
	CF_3Hg-F-actin	0.5 and 5 kHz	41 ppm
	CF_3Hg-G-actin	1 kHz	
	CF_3Hg-F-actin-S1	5 kHz	
PFPITC	PFPITC-*Lys* (dry)	3 kHz (3 peaks)	−70, −80, −87 ppm
	PFPITC-*Lys* (wet)	0.5 kHz	
	PFPITC-F-actin	3 kHz (3 peaks)	

F-actin filament. The Stokes-Einstein expressions is given in (3):

$$\tau_c = 4\pi\eta r^3/3kT \quad (3)$$

where the viscosity of the G-actin solution $\eta = 1.1 \times 10^{-3}$ Ns m^{-2} and the radius r is assumed to be half the longest dimension of the monomer, 3.4 nm (Kabsch et al. 1985). Equation (3) yields a value of 42 ns, in good agreement with the range determined experimentally (Barden and Phillips 1990).

The expression for the diffusion of a rigid rod about its long axis (Broersma 1960) was used to model the F-actin filament:

$$\tau_c = 4\pi\eta r^2 l/kT \quad (4)$$

where l is the filament length. For $l = 1$ μm, $\tau_c = 38$ μs.

A comparison of the times derived from (3) and (4) with the experimentally determined values indicates that for G-actin, the τ_c (CF_3Hg-actin) = 3.7 ns is indistinguishable from that of the Met εCH_3. This correlation time is an order of magnitude faster than monomer tumbling and presumably is due to some rapid internal motion. Similarly, the values of τ_s (BTFP-F-actin) and τ_s (CF_3Hg-F-actin) of 8 and 7 μs respectively are 4–5 times faster than for F-actin tumbling and can be attributed to internal motion such as domain twisting. These values compare well with those derived using IAEDANS (Ikkai et al. 1979) and ε-ADP (Mihashi and Wahl 1975) on F-actin.

A distinct relationship between probe size and τ_c is obtained with samples of labeled G-actin implying that the motion to which the probe is sensitive is affected by the probe bulk. The motion leading to values of $\tau_c = 42$ ns, measured with an immobile probe on the monomer (Barden and Phillips 1990) reflect overall monomer rotation. Values as low as 3.7 ns obtained in this study and 7 ns (Waring and Cooke 1987) reflect motion such as domain oscillation which is sensitive to steric effects imposed by the probes. The fluorescent studies of F-actin show some mobility on the nanosecond timescale which is probably attributable to monomer rotation (Mihashi and Wahl 1975). The timescale of filament motion as a whole is of the order of microseconds. Not surprisingly, there is no direct relation between correlation time and probe size. A more likely influence on the correlation time is the effect of a label on the intramonomer co-ordination or segmental mobility. The correlation times determined in the current work using pelleted samples were 4–5 times shorter than the value derived theoretically. Comparing these results with the only other reported study of pelleted actin, a solution of oxyltetramethylpiperidinylmaleimide labeled F-actin, yielded a correlation time of 40 μs which increased to 100 μs when pelleted (Hegyi et al. 1988). In the present study, solid state NMR is used to probe the aggregated filaments of F-actin within the highly concentrated pellets using two probes of similar size. There is little difference in the values of τ_c. Similarly, the binding of S-1 to F-actin followed by the pelleting of the complex did not alter the correlation time. The only evidence obtained of a change in protein dynamics during aggregation was the disappearance of the sharp spike in the CF_3Hg-F-actin pellet over several days. The solution state NMR measurements are performed at much lower protein concentrations and are capable of sensing the nanosecond dynamics of the monomer and small filaments but fail to report on the microsecond time scale discussed here (Barden et al. 1989; Barden and Phillips 1990).

The molecular dynamics of actin in all states of aggregation from monomeric G-actin to large filamentous complexes is sensed by the motion of the attached probes. The present study revealed no significant difference between the correlation times of F-actin and F-actin-S1 pellets in the time scale of the solid state experiment. A similar value was reported with the F-actin-Tm-Tn complex (Mihashi and Wahl 1975).

The linewidths of the resonance signals at half height are presented in Table 2. The d_2-IAA dry powder produced a rigid lattice powder spectrum with quadrupole

splitting of 165 kHz between the 90° edges (Fig. 2b). By contrast, freeze-dried d_2-IAA-labeled actin (Fig. 3a) gave a deuterium NMR spectrum indicative of a two-fold flip of the IAA group. When hydrated, a component (<25%) of the probe species underwent rapid disordered motion (Fig. 3b) which could be frozen out at low temperature (Fig. 3c). The restricted motion seen from the d_2-IAA-labeled actin was further evidence of the high order present in actin adjacent to the *Cys*-374 and *Cys*-10 sites. However, the poor signal/noise ratio obtained from the d_2-IAA probe led to the present study emphasising the ^{19}F probes.

A comparison of the linewidths and the T_2 measurements reported in Table 1 reveal that the linewidth of the ^{19}F *Cys* probes may be accounted for by relaxation effects. This is expected if the central peak is dominated by the $I=+1/2$ to $I=-1/2$ transition for an isolated and rapidly reorienting CF_3 group. However, the data obtained for the CF_3Hg-labeled F-actin samples have static contributions beyond that due to relaxation. These contributions may be due to variations in rigid lattice interactions or they may arise from F–H dipolar interactions with adjoining molecular groups. Taking into account the order of the surrounding species and the CF_3 rotor axis, these contributions may account for the differences in linewidth (Seiter and Chan 1973; Post et al. 1984).

The dynamics of the probes attached to either dry cysteine powder or F-actin have been shown to be very similar in this study. The probes on G-actin appear to sense monomer rotation. The results indicate that there is little change in the dynamics when myosin S1 binds to F-actin and the complex is pelleted. Thus, the dynamics of the probe sites *Cys*-10 and *Cys*-374 on pelleted F-actin appear to be dominated by the local environment and are little influenced by external interactions such as myosin binding.

Acknowledgements. This work was supported by grants from the National Health and Medical Research Council of Australia and the Clive and Vera Ramaciotti Foundation. The authors wish to thank Mr. Frank Crino for assistance in running the CXP-300 spectrometer.

References

Andrew ER, Bersohn R (1950) Nuclear magnetic resonance line shape for a triangular configuration of nuclei. J Chem Phys 18:159–161

Barden JA, dos Remedios CG (1985) Conformational changes in actin resulting from the Ca^{2+}/Mg^{2+} exchange as detected by proton NMR spectroscopy. Eur J Biochem 146:5–8

Barden JA, Phillips L (1990) ^{19}F NMR study of actin modified at *Lys*-61 with pentafluorophenylisoythiocyanate. Biochemistry 29:1348–1354

Barden JA, Cooke R, Wright PE, dos Remedios CG (1980) Proton NMR and EPR studies on skeletal muscle actin indicates that the metal and nucleotide binding sites are separate. Biochemistry 19:5912–5916

Barden JA, Symons P, Cartmill PA, Miki M, Hambly BD (1986a) Extraction of myosin light chains and actin from bovine cardiac muscle acetone powder. Anal Biochem 158:288–293

Barden JA, Miki M, dos Remedios CG (1986b) Selective labelling of *Cys*-10 on actin. Biochem Int 12:95–101

Barden JA, Phillips L, Cornell BA, dos Remedios CG (1989) ^{19}F NMR studies of the interaction of selectively labeled actin and myosin. Biochemistry 28:5895–5901

Bendall MR, Lowe G (1976) ^{19}F NMR probes for proteins; *S*-trifluoromethylmercuripapain. FEBS Lett 72:231–234

Brauer M, Sykes BD (1981a) Phosphorus-31 nuclear magnetic resonance studies of the adenosine 5'-triphosphate-Ca-G-actin complex. Biochemistry 20:2060–2064

Brauer M, Sykes BD (1981b) Proton-NMR studies of ATP bound to a nitrated derivative of G-actin. Biochemistry 20:6767–6774

Brauer M, Sykes BD (1986) ^{19}F nuclear magnetic resonance studies of selectively fluorinated derivatives of G- and F-actin. Biochemistry 25:2187–2191

Broersma S (1960) Rotational diffusion constant of a cylindrical particle. J Chem Phys 32:1626–1631

Doddrell D, Glushko V, Allerhand A (1972) Theory of nuclear Overhauser enhancement and ^{13}C-^1H dipolar relaxation in proton-decoupled carbon-13 NMR spectra of macromolecules. J Chem Phys 56:3683–3689

Erickson HP (1989) Co-operativity in protein-protein association. The structure and stability of the actin filament. J Mol Biol 206:465–474

Forsén S, Lindman B (1981) Ion binding in biological systems as studied by NMR spectroscopy. Methods Biochem Anal 27:289–486

Frieden C (1982) The Mg^{2+}-induced conformational change in rabbit skeletal muscle G-actin. J Biol Chem 257:2882–2886

Habeeb AFSA (1972) Reaction of protein sulfhydryl groups with Ellman's reagent. Methods Enzymol 25:457–464

Hambly BD, Barden JA, Miki M, dos Remedios CG (1986) Structural and functional domains on actin. BioEssays 4:124–128

Hegyi G, Szilagyi L, Belagyi J (1988) Influence of the bound nucleotide on the molecular dynamics of actin. Eur J Biochem 175:271–274

Ikkai T, Wahl P, Auchet J-C (1979) Anisotropy decay of labelled actin. Eur J Biochem 93:397–408

Jacobs WA, Heidelberger M (1932) Chloroacetamide. Organic Syntheses Collective 1:153–154

Kabsch W, Mannherz HG, Suck D (1985) Three-dimensional structure of the complex of actin and DNase I at 4.5 A resolution. EMBO J 4:2113–2118

Kamenar B, Korpar-Colig B, Hergold-Brundic A, Popovic Z (1982) Structure of bis(trifluoromethyl)mercury II-2,2':6',2''-terpyridyl. Acta Crystallogr B38:1593–1595

Kinsey RA, Kintanar A, Oldfield E (1981) Dynamics of amino acid side chains in membrane proteins by high field solid state deuterium nuclear magnetic resonance spectroscopy. J Biol Chem 256:9028–9036

Korn ED (1982) Actin polymerization and its regulation by proteins from non-muscle cells. Physiol Rev 62:672–737

Kurzer F, Lawson A (1963) Methylisourea hydrochloride. Organic Syntheses Collective 4:645–649

Matthews HR, Matthews KS, Opella SJ (1977) Selectively deuterated amino acid analogues. Synthesis, incorporation into proteins and NMR properties. Biochim Biophys Acta 497:1–13

Mejean C, Hue HK, Pons F, Roustan C, Benyamin Y (1988) Cation binding sites on actin: A structural relationship between antigenic epitopes and cation exchange. Biochem Biophys Res Commun 152:368–375

Mihashi K, Wahl P (1975) Nanosecond pulse fluorometry in polarized light of G-actin-ε-ATP and F-actin-ε-ADP. FEBS Lett 52:8–12

Miki M, Barden JA, dos Remedios CG, Phillips L, Hambly BD (1987) Interaction of phalloidin with chemically modified actin. Eur J Biochem 165:125–130

Miller L, Kalnowski M, Yunossi Z, Bulinski JC, Reisler E (1987) Antibodies directed against N-terminal residues on actin do not block acto-myosin binding. Biochemistry 26:6064–6070

Mossakowska M, Belagyi J, Strzelecka-Golaszwska H (1988) An EPR study of the rotational dynamics of actins from striated and smooth muscle and their complexes with heavy meromyosin. Eur J Biochem 175:557–564

Oosawa F (1983) Macromolecular assembly of actin. In: Stracher A (ed) Muscle and nonmuscle motility, vol 1. Academic Press, New York, pp 115–216

Pines A, Gibby MG, Waugh JS (1973) Proton enhanced NMR of dilute spins in solids. J Chem Phys 59:569–590

Post JFM, Cottam PF, Simplaceanu V, Ho C (1984) Fluorine-19 nuclear magnetic resonance study of 5-fluorotryptophan-labelled histidine-binding protein of *salmonella typhimurium*. J Mol Biol 179:729–743

Sarkar S, Hayama Y, Niu CH, Young PE, Jerig JT, Torchia DA (1987) Molecular dynamics of collagen sidechains in hard and soft tissues. A multinuclear magnetic resonance study. Biochemistry 26:6793–6800

Seiter CHA, Chan SI (1973) Molecular motion in lipid bilayers. A nuclear magnetic resonance line width study. J Am Chem Soc 95:7541–7553

Spiess HW (1984) Characterization of polymers in the solid state I. In: Kausch HH, Zachmann HG (eds) Advances in Polymer Science, vol 66. Springer, Berlin Heidelberg New York, pp 23–59

Sutoh K (1982) Identification of myosin binding sites on the actin sequence. Biochemistry 21:3654–3661

Sutton LE (ed) (1958) Tables of interatomic distances and configurations in molecules and ions. The Chemical Society, London

Tonomura Y, Appel P, Morales MF (1966) On the molecular weight of myosin. Biochemistry 5:515–521

Vandekerckhove J, Deboben A, Nassal M, Wieland T (1985) The phalloidin binding site of F-actin. EMBO J 4:2815–2818

Vogel AI (1979) Vogel's textbook of quantitative inorganic analysis. Wiley, New York. pp 193, 367–369, 403, 428–429

Waring AJ, Cooke R (1987) The molecular dynamics of actin measured by a spin probe attached to lysine. Arch Biochem Biophys 252:197–205

Weeds AG, Taylor RS (1975) Separation of subfragment-1 isoenzymes from rabbit skeletal muscle myosin. Nature 257:54–56

Woessner DE (1962) Spin relaxation processes in a two-proton system undergoing anisotropic reorientation. J Chem Phys 36:1–4